Applied Mathematics and Mechanics
(English Edition, Vol. 19, No. 1, Jan. 1999)

Published by SU,
Shanghai, China

A COUPLING MODEL FOR TERRESTRIAL PROCESSES IN ARID AREAS AND ITS APPLICATION *

Li Jiachun(李家春), Yao Deliang(姚德良)
Shen Weiming(沈卫明), Xie Zhengtong(谢正桐)
Institute of Mechanics, CAS, Beijing 100080, P. R. China

(Received April 14, 1997; Revised Aug. 28, 1998)

Abstract: *In this paper, the importance of investigation on terrestrical processes in arid areas for mankind's living environment protection and local economy development as well as its present state of the art are elucidated. A coupling model, which evaluates heat, mass, momentum and radiative fluxes in the SPAC system, is developed for simulating microclimate over plant and bare soil. Especially, it is focussed on the details of turbulence transfer. For illustration, numerical simulation of the water-heat exchange processes at Shapotou Observatory, CAS, Ninxia Province are conducted, and the computational results show that the laws of land-surface processes are rather typical in the arid areas.*

Key words: coupling model; land-atmosphere interaction; turbulent model

Introduction

It is well-known that land-atmosphere interaction exerts great influences on global and regional environment (Wood 1991, Yih 1994). In order to determine the fluxes and the parameterization scheme at the land-atmosphere interface, it is necessary for us to investigate terrestrial processes on typical underlying surface. Arid area (including extremely arid, arid and semi-arid areas) of 48 million km^2, occupies almost one third of the land surface, mainly in North Africa, Central Asia, Australia and North America. Among them desert covers nearly 6 million km^2 (Wu 1987). The role of the arid area is considerably important for global circulation due to high albedo (up to 35%), large Bowen ratio, small evaporation and stratification.

It is reported by UNEP that desertification occurs at the rate of approximately 6 million hectares annually owing to world-scale climatic changes and overgrazing of land, which indeed threatens the sustainable development of world economy and the future life of mankind. Men have come to recognize that desertification is an extremely serious problem to the world. The arid and semi-arid environmental system is very sensitive to the changes due to natural evolution and anthropogenic activities. It is most important to protect the environment at the juncture of arid and humid area (Zhu 1994). As an example, Xinjiang as the largest province in China, is rich in mineral resources such as petroleum, gas and metals. Although local precipitation sems little, there is enough sunshine and water from precipitation in mountain areas and melted snow. However, although we have cultivated a large expanse of oasis, a great many environmental problems such as shrinking of rivers, drying of lakes, degeneration of pasture, desertification of land etc.

* Project supported by CNSF, CSA, Shapotou Observatory and LNM

occur (Wu 1992). An additional example is the "San Bei" windbreak aiming to protect the railway from being buried by sand coming from the desert. About three decades ago, a few kinds of drought-enduring plants successfully survived by cellular straw technique at the south border of the Tenggeli desert. During the infant stage, they grew normally, thus resulting in the formation of a windbreak belt to hinder the movement of the desert. Nevertheless, these plants started to wither due to the increase of water demand and the existence of biological skin. Hence, the study of energy and water cycling is certainly beneficial to preventing land from desertification, improving environmental quality and developing regional economy.

A great improvement such as prescribing soil potential temperature and proposing Bucket Model, was made to understand land-atmosphere interaction and land-surface parameterization scheme. Since early 1980s, canopy biophysical and physiological processes for water and heat cycling are extensively studied. A few models for SPAC system, such as BATS model (Dickinson 1986) and SIB model (Seller 1986) have been proposed. On the other hand, atmospheric turbulence transfer is fundamentally decisive to momentum, mass and energy exchange. Scientists have paid attention to coupling models for simulating the land - atmosphere interaction as a result. Naot (1989) has developed a second-order model to simulate the micrometeorology in cotton fields and bare soil at Nahal-Oz and Gilgal, Israel. The paper was mainly a verification of numerical simulation with the micrometeorology parameters (temperature, humidity, velocity, et al.) at the height of 4 meter above the soil surface at every time step specified. Generally speaking, the underlying surface in a single grid of the GCM is nonhomogeneous, there always scatter farm land, forests, grass land, lakes, bogs, hills, oasises and cities on the earth. On this account , the study on land - surface parameterization over nonhomogeneous surface is of conside - rable significance to improving GCM. During the last decade, several international co-operation of observations were conducted to address to the problem of estimating area - averaged surface flu - xes over homogeneous terrain. The main thrust of the HAPEX-MOBILHY and HIFE experimental programs were towards investigating techniques involved in integrating the turbulent surface fluxes measured in local sites to a large scale approaching that used in GCM. HEIFE was carried out in the arid area of Northwest China with complex surface codition, its main objectives are identified as: to collect comprehensive data sets and obtain better understanding of land surface processes, to test and improve the parameterization scheme of energy and water budgets at a grid scale of mid-latitude arid zones, to improve the utilization of water resources in this area based on a better understanding of area hydrological processes and so on.

In this paper, we show how the conservation equations for heat, moisture and momentum and their corresponding fluxes in the low atmosphere can be coupled with soil water and heat transfer to simulate the detailed micrometeorology , considering the influence of sparse drought - enduring plants . We carefully study the water and heat exchange in arid area , aiming at protec - ting " San Bei " windbreak . Comparisons are made between the measured and the calculated pro - files of hourly averaged temperature , net radiation and humidity and the like . Field observation is conducted simultaneously at the Shapoutou Observatory, Ninxia province.

1 Coupling Model

Based on the land-surface processes model suggested by Ten Berge (1990), we further con-

sider the influences of drought-enduring plants in desert. This work is applied to water-energy cycling research on "San Bei" windbreak area. Different from so called "Forced Restore Method", the temperature, moisture and wind profiles are calculated as results in the present model, but need not be given as boundary conditions.

1.1 Turbulence Movement in ABL

Generally speaking, the flows in ABL are fully-developed turbulent, which can be described by the Reynolds averaged Navier-Stokes equation including rotation and stratification effects. Since the horizontal pressure gradient can be represented by the geostrophic wind u_g, v_g, the governing equations for a horizontally homogeneous flow are written as:

$$\frac{\partial \bar{u}}{\partial t} = f(\bar{v} - v_g) - \frac{\partial}{\partial z}\left(\frac{\tau_x}{\rho}\right), \tag{1 a}$$

$$\frac{\partial \bar{v}}{\partial t} = -f(\bar{u} - u_g) - \frac{\partial}{\partial z}\left(\frac{\tau_y}{\rho}\right), \tag{1 b}$$

$$\frac{\partial \bar{T}}{\partial t} = -\frac{\partial}{\partial z}\left(\frac{H}{\rho C_p}\right), \tag{1 c}$$

$$\frac{\partial \bar{q}}{\partial t} = -\frac{\partial}{\partial z}\left(\frac{E}{\rho}\right), \tag{1 d}$$

$$\frac{\partial e}{\partial t} = \frac{\tau_x}{\rho}\frac{\partial \bar{u}}{\partial z} + \frac{\tau_y \partial \bar{v}}{\rho \partial z} + \frac{g}{T}\frac{H}{\rho C_p} + \frac{\partial}{\partial z}\left(K_M \frac{\partial e}{\partial z}\right) - \frac{(Ce)^{3/2}}{l_M}, \tag{1 e}$$

where $\bar{u}$, $\bar{v}$ are the averaged velocities in x, y directions, $\bar{T}$, $\bar{q}$ are mean potential temperature and specific humidity, t is the time, z is the vertical coordinate. $f = 2\Omega\sin\phi$ is the Coriolis parameter. $\Omega = 7.27 \times 10^{-5}/\mathrm{s}$, ϕ is the local latitude, ρ is the density of atmosphere, C_p is the heat capacity, g is the acceleration due to gravity, e is the turbulent kinetic energy (TKE ; $e = 0.5(u'^2 + v'^2 + w'^2)$). τ_x, τ_y, H, E are Reynolds stresses, sensible heat fluxes, latent heat fluxes, which can be written as follows:

$$\frac{\tau_x}{\rho} = \overline{u'w'} = -K_M \frac{\partial \bar{u}}{\partial z}, \tag{2a}$$

$$\frac{\tau_y}{\rho} = \overline{v'w'} = -K_M \frac{\partial \bar{v}}{\partial z}, \tag{2b}$$

$$\frac{H}{\rho C_p} = \overline{T'w'} = -K_H \frac{\partial \bar{T}}{\partial z}, \tag{2c}$$

$$\frac{E}{\rho} = \overline{q'w'} = -K_V \frac{\partial \bar{q}}{\partial z}. \tag{2d}$$

We apply K model to close the foregoing equation system . The total transfer coefficient can be expressed as a function of TKE

$$K_{M,H,V} = l_{M,H,V}(Ce)^{1/2}, \tag{3a}$$

and

$$l_{M,H,V}^{-1} = \frac{\psi_{M,H,V}(\zeta)}{kz} + \frac{f}{\alpha u_g}, \tag{3b}$$

where $\alpha = 4.0 \times 10^{-4}$, $c = 0.2$ are empirical constant, k is the von-Karman constant taken as 0.41, and ψ is the stability function,

$$\psi_M = \begin{cases} (1 - 16\zeta)^{-1/4} & \text{for unstable stratification} \\ 1 & \text{for neutral condition} \\ (1 + 4.7\zeta) & \text{for stable stratification,} \end{cases} \tag{4a}$$

$$\psi_V = \psi_H = \begin{cases} (1 - 16\zeta)^{-1/2} & \text{for unstable stratification} \\ 1 & \text{for neutral condition} \\ (1 + 4.7\zeta) & \text{for stable stratification,} \end{cases} \tag{4b}$$

where $\zeta = Z/L$, L is the well-known Monin-Obukhov, length, defined as

$$L = \frac{T(\tau/\rho)^{3/2}}{kg(H/\rho C_p)}. \tag{5}$$

The conditions at the upper boundary of the system are defined as is below,

$$\tau_x = \tau_y = 0, \tag{6a}$$

$$H = 0, \tag{6b}$$

$$E = 0, \tag{6c}$$

$$\frac{\partial e}{\partial z} = 0. \tag{6d}$$

The lower boundary conditions to the atmosphere, dictated by the surface energy balance, have been treated in the subsection 1.3.

1.2 Water and heat transfer in the soil

The one-dimensional flow equation for heat in the soil can be written as

$$\frac{\partial (CT)}{\partial t} = \frac{\partial}{\partial z}\left(\lambda \frac{\partial T}{\partial z}\right), \tag{7}$$

where T is the soil temperature, C is the volumetric heat capacity, λ is thermal conductivity. Both the thermal conductivity and heat capacity can be formulated on the basis of soil composition

$$C = f_q c_q + f_c c_c + f_o c_o + \theta c_w + f_a c_a, \tag{8}$$

where f is the volume fraction and C is the volumetric heat capacity of the components clay, quartz, organic matter, water and air, respectively; θ is the volume fraction of soil water

$$\lambda = \begin{cases} \dfrac{k_{qw} f_q \lambda_q + k_{cw} f_c \lambda_c + k_{ow} f_o \lambda_o + k_{ww} \theta \lambda_w + k_{aw} f_a \lambda_a}{k_{qw} f_q + k_{cw} f_c + k_{ow} f_o + k_{ww} \theta + k_{aw} f_a} & (\theta > 0.05), \\ 1.25 \dfrac{k_{qa} f_q \lambda_q + k_{ca} f_c \lambda_c + k_{oa} f_o \lambda_o + k_{wa} \theta \lambda_w + k_{aa} f_a \lambda_a}{k_{qa} f_q + k_{ca} f_c + k_{oa} f_o + k_{wa} \theta + k_{aa} f_a} & (\theta < 0.02). \end{cases} \tag{9}$$

For $\theta > 0.05$, the liquid is used as the continuous phase, the weighting factors k_{qw}, k_{cw}, k_{ow} and k_{aw} depend on the ratio of specific thermal conductivity of quartz, clay, organic matter, and air to that of water respectively. At very low water contents ($\theta < 0.02$), air is viewed as the continuous phase.

For component x in medium y in the direction i, k_{xy} is defined as

$$k_{xyi} = \frac{1}{1 + \left(\frac{\lambda_x}{\lambda_y} - 1\right) g_{xi}}, \tag{10}$$

where g_{xi} is the shape factor for direction i of the particle. If the particle axis has random directions in the bulk soil, the weight factors are expressed as

$$k_{xy} = \frac{1}{3}[k_{xy1} + k_{xy2} + k_{xy3}], \tag{11a}$$

and for spheroids, it results in

$$k_{xy} = \frac{2}{3}\Big/\left(1 + \left(\frac{\lambda_x}{\lambda_y} - 1\right)\right) g_{xi} + \frac{1}{3}\Big/\left(1 + \left(\frac{\lambda_x}{\lambda_y} - 1\right)\right)(1 - 2g_{xi}), \tag{11b}$$

where $i = 1$, $g_a = 0.2$, $g_c = 0.01$, $g_o = 0.5$, $g_q = 0.14$, $g_w = 0.14$.

The general flow equation for one-dimensional transport of liquid water in the soil is written as,

$$\rho_1 \frac{\partial \theta}{\partial t} = \frac{\partial}{\partial z}\left(K(\theta, T)\frac{\partial p(\theta, T)}{\partial z}\right) - \rho_1 g \frac{\partial}{\partial z} K(\theta, T), \tag{12}$$

where ρ_1 is the density of liquid water, θ is the volumetric water content, K is the hydraulic conductivity, p is the pressure potential, g is the gravity acceleration. The pressure potential can be defined as

$$p = -\frac{1}{\alpha}(\xi^{-\frac{1}{m}} - 1)^{\frac{1}{n}}, \tag{13}$$

where $m = 1 - (1/n)$, $\xi = (\theta - \theta_r)/(\theta_s - \theta_r)$, and θ_r, θ_s are the residual moistrue content and the moisture content at saturation, respectively, α, n are empirical constants. The hydraulic conductivity can be written as

$$K = K_s \xi^{\frac{1}{2}}[1 - (1 - \xi^{\frac{1}{m}})^m]^2, \tag{14}$$

where K_s is the hydraulic conductivity at saturation. K is taken as zero for $\theta < \theta_r$.

The conditions at the lower boundary of this system are defined as is given below,

$$\frac{\partial T}{\partial z} = \frac{\partial \theta}{\partial z} = 0.$$

1.3 The surface energy balance

The central equation that sets boundary conditions to the soil and the atmosphere subsystems is the energy balance equation of the surface

$$R_n + H + LE = G, \tag{15}$$

where R_n, H_s, E_s, G are net radiation, sensible and latent heat fluxes and soil heat flux respectively, all in Wm^{-2}. This equation implies that as the surface itself has no capacity, no energy can be stored in it.

A complication that should be mentioned explicitly in this context is the relation between G

and soil surface condition, for example, the net radiation is related to the soil temperature and soil moisture, sensible and latent heat fluxes rely on the soil temperature, moisture, atmosphere temperature and transfer coefficient, which depends on wind velocity, surface roughness, atmosphere stability.

The net radiation is written as follows

$$R_n = (1 - a)R_{glob} + R_{le} + (1 - \varepsilon)R_{ld}, \tag{16}$$

where R_{glob} is the global radiation, R_{le} is the surface longwave radiation, R_{ld} is the sky longwave radiation, α is the albedo, ε is the surface emissivity.

As the albedo α is also dependent on the position of the sun and the atmospheric conditions, we focus on the influence of the surface condition. The effect of moisture on albedo is marked. The linear relationship between albedo α and volumetric soil moisture content θ has been adopted:

$$a(\theta) = a_{wet} + \frac{\theta_{crit} - \theta}{\theta_{crit}}(a_{dry} - a_{wet}). \tag{17}$$

In practice, the longwave radiation is often taken to be a function of air temperature at screen height (1.5m):

$$R_{ld} = \varepsilon_{sky}\sigma T_a^4, \tag{18}$$

where $\sigma = 5.67 \times 10^{-8}\mathrm{W/m^2K^4}$ is the Stefan-Boltzmann constant, ε is the sky emissivity, which is formulated as

$$\varepsilon_{sky} = a + b\sqrt{e}, \tag{19a}$$

where e is the vapor pressure at screen heigt (hpa), a, b are constant. For cloudy skies, the sky emissivity can be written as,

$$\varepsilon_{sky}(n) = \varepsilon_{sky}(0)(1 + nc^2), \tag{19b}$$

where n is a parameter ranging from 0.04 for high (cirrus) cloud, to 0.2 for low cloud, c is the fraction of cloud cover.

The surface emissivity is defined as follows

$$R_{le} = -\varepsilon\sigma T_s^4, \tag{20a}$$

where T_s is the soil surface temperature

$$\varepsilon(\theta) = \varepsilon_{dry} + \frac{\theta}{\theta_s}(\varepsilon_{wet} - \varepsilon_{dry}), \tag{20b}$$

where ε ranges from 0.9 to 1.0. Although differences in soil emissivity are hardly significant in the energy balance, they are of course important in the interpretation of thermal infrared imagery.

2 Field Observation

The Shapotou Experimental Observatory, located at 37°27′N, 104°57′E with elevation 1250 meters ASL, belongs to semidesert areas of the northwest inner land with hot, dry and windy climate. Climate conditions are of continental monsoon type with annual mean temperature 9.6℃, the annual mean precipitation of 177.3mm. Temperature changes drastically from day to night and from summer to winter, and the precipitation is unevenly distributed seasonally, so the shortage of moisture is a severe problem there. The annual mean wind velocity is 2.8m/s with the largest 19m/s, there are about 200 days when the wind velocity is greater than 5m/s, and the

disaster of sand flows is also severe. The local soil is fine sand, containing little organic matter, where plants can hardly live. There is little vegetation coverage of less than 1% ~ 2% because the natural conditions are unfavourable for plants to grow owing to deep underground water table and worse water-holding ability of sandy soil (usually water capacity is 2% ~ 3%).

Since 1950s, Shapotou Observatory has taken mechanical and biological measures, such as setting up sand barriers and planting drought endurable plants by the cellular straw technique, to fix flowing sand. A few kinds of drought-enduring plants such as Hedisarum scoparium, Caragana korshinskii and Artemisia ordosica et al. successfully survived, and a 16km long windbreak belt was formed to protect the Bao-Lan railway during Gantang and Zhongwei. Nevertheless, the water demand increases with the growing of these plants, and a kind of biological skin was formed such that these plants started to wither.

In order to estimate various microclimate parameters and verify the present model, we conducted a field observation in the Shapotou region, Ningxia Province during September, 1993. The site of measurement was located near the micrometeorology observatory, where the mean canopy height was 1 meter, plants coverage ratio 30%. Experimental data included hourly measurements of temperature, humidity (by Asimann ventilated psychrometer), wind speed (by cup anemometer), the heights of measurement are 1, 2, 4, 8, 16 meter, respectively. Besides these conventional meteorological measurement, some special measurements were conducted, such as net radiation (by CN-1 net pyrradiometer made in Australia, the height of measurement 2m), soil heat flux (by CN-3 Thermal Flux Plate buried at the depth 1 cm), evapotranspiration (by Lysimeter), soil moisture (by baking and weighing method) and soil temperature (measured at 5, 10, 20, 40, 60, 80, 100, 125, 150, 175, 200cm depths).

3 Results and Discussion

To verify the feasibility of the present model, numerical simulation for turbulent flow of

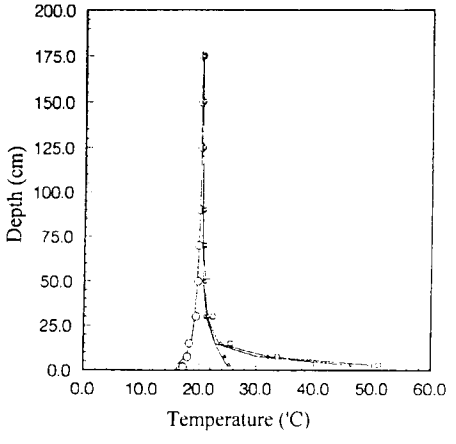

Fig. 1(a) Soil temperature profiles at the time of 8:00, 20:00, 12:00 and 16:00 from left to right

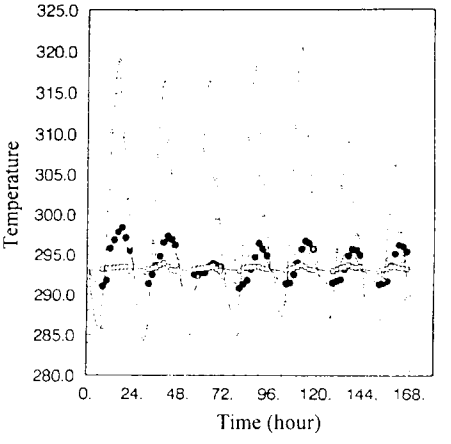

Fig. 1(b) The variations of temperature at the depth of 0 cm, 10 cm and 100 cm with time from top to bottom

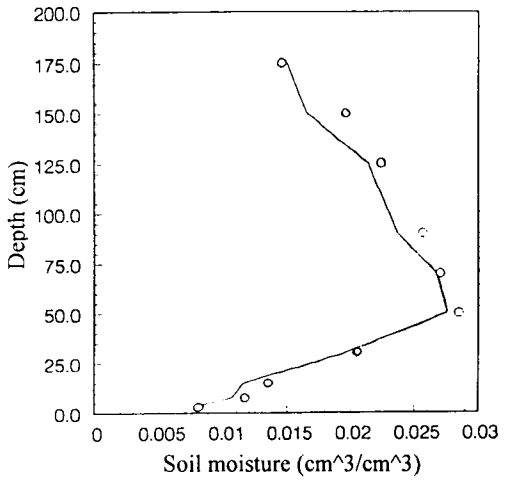

Fig. 2(a) Soil moisture profile

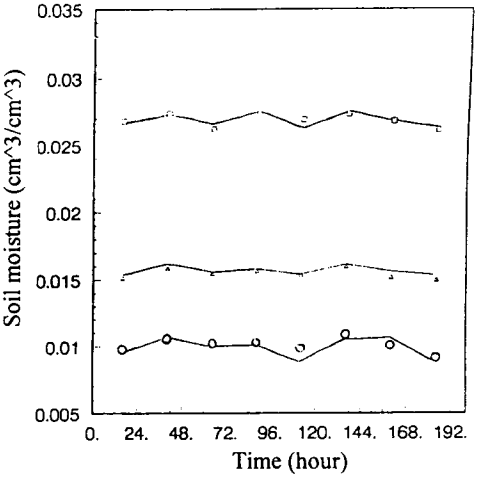

Fig. 2(b) The variations of moisture at the depth of 50cm, 100cm, 5cm from top to bottom

ABL and soil water and heat cycling in the Shapotou region of Ninxia Province was conducted. First of all, the meteorological data and some parameter have to be prescribed, such as radiation, precipitation, cloud cover, Coriolis parameter, roughness, geostrophic wind, soil component,

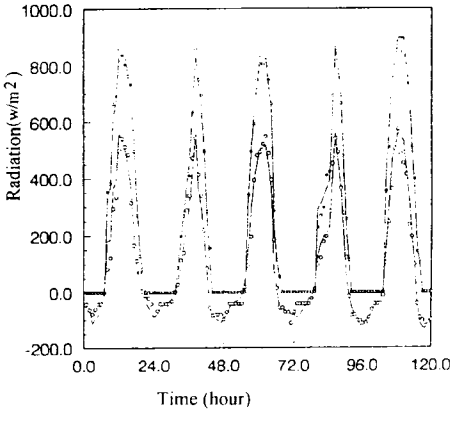

Fig. 3 The variations of the global and net radiation with time from top to bottom

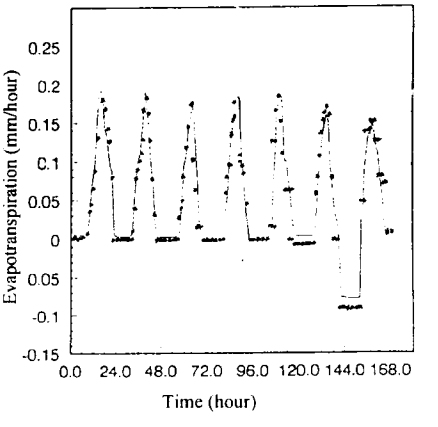

(—: represents simulated data, * : represents measured data)

Fig. 4(a) The variation of evapotranspiration with time

heat capacity, thermal conductivity, shape factor, hydraulic conductivity, albedo, emissivity, sky parameter and so on. Equations (1), (7) and (12) are numerically integrated by a finite-difference scheme, which are discretized in space by applying staggered grid control volume method with forward time step, ABL and soil are divided into 6 layers and 11 layers respectively. Nonlinear equation (15) is solved by the Newton iteration. Initial profiles of wind speed, air temperature and humidity, soil temperature and moisture should be given.

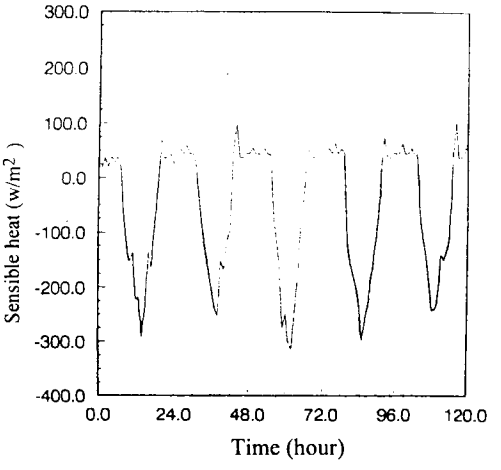

Fig. 4(b) .The variation of sensible flux with time

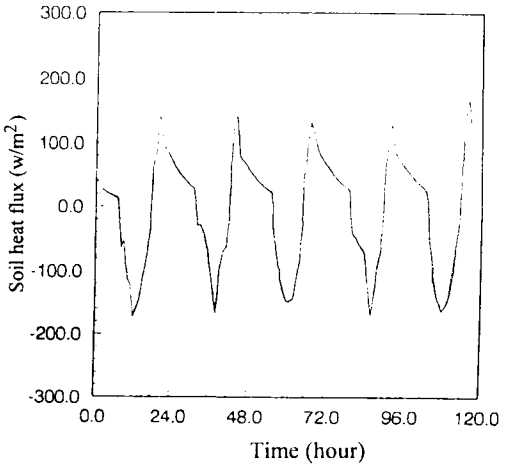

Fig. 4(c) The variation of soil heat heat with time

Fig. 1(a) shows calculated diurnal variation of soil temperature profiles. We find that in the arid area , the soil surface temperature changes drastically , and the highest amplitude reaches 30°C. The temperature reaches the lowest at 8:00 while the highest at 16:00. The temperature at deeper layers exhibits little variation. Fig. 1(b) illustrates the diurnal variations of calculated soil temperature at various depths, which agree well with that by "forced restore method".

Fig. 2(a) is the comparison of calculated and measured soil moisture profile. A dry sand layer with moisture of only around 1% exists at depth 6 ~ 7cm so that the maximum of moisture content occurs at the depth of 50cm or so. Another reason responsible for the phenomenon is that dry climate in the area results in fierce evaporation and water can not penetrate into very deep layer or even is entirely evaporated, so that the most humid layer exists in the middle at the depth of 50cm or so. Fig. 2(b) illustrates the diurnal variations of calculated soil moisture at various depths, which also agree well with that by "forced restore method".

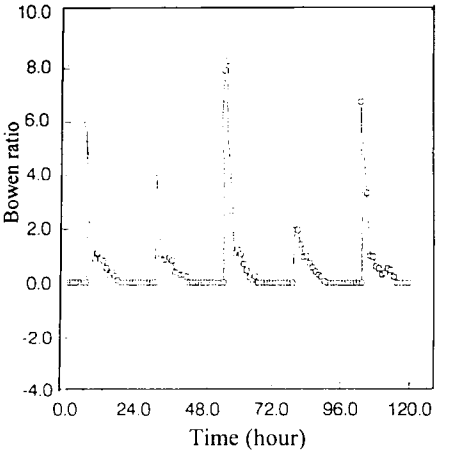

Fig. 5 The variation of bowen ratio with time

The diurnal variation of measured and calculated global and net radiation are depicted in Fig. 3. The diurnal global radiation reaches 20 million J/m^2 due to the strong sunshine in autumn, while the diurnal net radiation is 8 million J/m^2 smaller than that in humid area because of the large albedo and strong long wave emission. Fig. 4 (a) ~ (c) are the diurnal variation of evapotranspiration, sensible heat flux and soil heat flux. The net radiation is distributed at the above component with the ratio: less than 10% , 70% , 20% . Hence, the largest Bowen ratio in Fig. 5 reaches as high as 8.

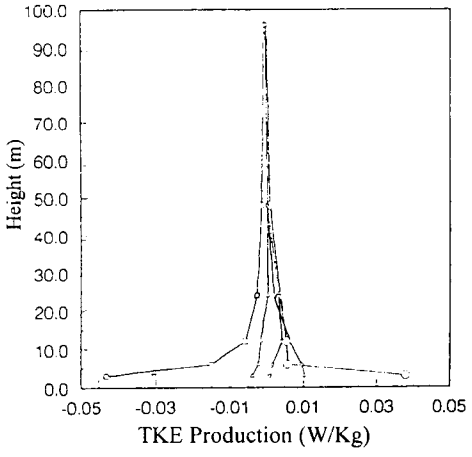

Fig. 6(a) TKE production profiles at 12:00

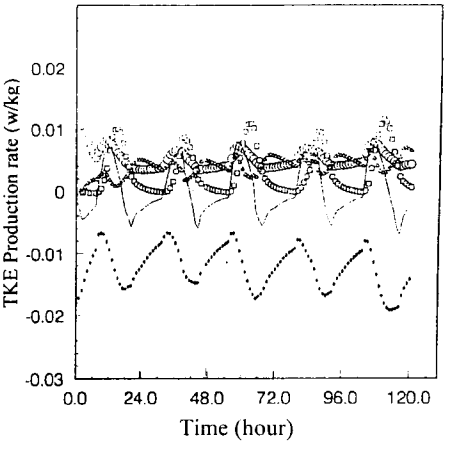

Fig. 6(b) The variation of TKE production rate at the depth of 2m with time

Fig. 6(a) shows profiles of TKE source/sink terms. We find that each term is rather large near the surface, especially for the shear production term (dot) and the TKE dissipation term (square). The production of buoyancy term (up-side-down triangle), the divergence term (lozenge) and the local rate of change of TKE (triangle) is also shown in Fig. 6(a). Fig. 6(b) illustrates the diurnal vriation of the TKE (line), shear production (dot), buoyancy production (square), divergence term and the dissipation term. Generally speaking, convective ABL make turbulence develop in the day time especially in the afternoon, while in the night, stable ABL tends to suppress the turbulence movement.

From the above results, we come to the conclusions as follows: the main terrestrial process in arid area is characterized by strong global radiation, large albedo, rather small net radiation, little evapotranspiration, large sensible heat flux, drastic surface temperature, and the stability of ABL exerts great influences on atmospheric turbulent flow and corresponding water and heat cycling in arid areas. These results agree well with observation in HEIFE (Hu, 1994). In a word, the mathematical model we have suggested can be used to simulate the energy and water cycling in arid areas so as to provide scientific foundation in the investigation of local ecological environment and parameterization for GCM.

References

[1] Chen Hesheng. Relation between growing plants in arid area and water balance [A]. Report of "75" National Science and Technology Key Research Item (75-08-01 – 06)[R]. 1990. (in Chinese)

[2] Hu Yingjiao, et al.. Some results of Heihe field observation [J]. *Plateau Meteo-rology*, 1994, **13**(3): 225 ~ 236. (in Chinese)

[3] Wu Shenyan. *Studies on Heat and Moisture Transfer in Tarim Basin* [M]. Beijing: Marine Publishing House, 1992. 1 ~ 9. (in Chinese)

[4] Wu Zheng. *Sand Flow Geomorphology* [M]. Beijing: Science Press, 1987, 1 ~ 17

[5] Ye Douzheng. Scientific Problem of Global Change [J]. *Atmospheric Science*, 1994, **18**

(4):498 ~ 512. (in Chinese)

[6] Zhu Zhengda. Present situation and prospects for the desertification [J]. *Geography Research*, 1994, **13**(1):104 ~ 113. (in Chinese)

[7] Dickinson R W, et al.. Biosphere-Atmosphere Transfer Scheme(BATS) for NCAR Community Model[A]. NCAR, Boulder Co., TN-275 + STR(R), 1986

[8] Li J C, et al. Studies on terrestrical interface processes in arid areas [A]. Technical Report, IMCAS STR-95008(R), 1995

[9] Mahrer Y, Pielke R A. Numerical simulation of the air flow over Barbados [J]. *Mon Wea Rev*, 1976, **104**: 1392 ~ 1402

[10] Naot O, Mahrer Y. Modelling microclimate environments: a verification study [J]. *Boundary Layer Meteorology*, 1989, **46**:333 ~ 354

[11] Seller P J, Mintz Y. A simple bioshere(SiB) for use within general circulation models [J]. *J Atmos Sci.*, 1986, **43**: 505 ~ 531

[12] Ten Berge H F M. *Heat and Water Transfer in Bail Topsoil and the Lower Atmosphere* [M]. Pudoc, Netherland, 1990

[13] Wood E F. *Land Surface-Atmosphere Interactions for Climate Modeling* [M]. Dordrechet: Kluwer Academic Publishers, 1991. 85 ~ 126, 155 ~ 178